Numerical investigation of the performance of a pile-restrained WEC-type dual-floating breakwater system

Haoyu Ding[1], Jun Zang[1*], Chris Blenkinsopp[1], Dezhi Ning[2], Xuanlie Zhao[2], Qiang Chen[1], Junliang Gao[1, 3],

1. Research Unit for Water, Environment and Infrastructure Resilience (WEIR), Department of Architecture and Civil Engineering, University of Bath, BA2 7AY, U.K.
* E-mail: J.Zang@bath.ac.uk.

2. State Key Laboratory of Coastal and Offshore Engineering, Dalian University of Technology, Dalian, 116024, China

3. School of Naval Architecture and Ocean Engineering, Jiangsu University of Science and Technology, Zhenjiang 212003, China

HIGHLIGHTS

This paper evaluates the performance of a pile-restrained WEC-type dual-floating breakwater system, which is a multi-functional integrated system consisting of wave energy converter (WEC) and floating breakwater. The investigation is conducted in a two-dimensional numerical wave tank based on the OpenFOAM® package.

1 INTRODUCTION

The integrated WEC-type of breakwater system considered in this paper is a multi-functional system, which aims to reduce the construction-cost and save construction-space. The concept of pile-restrained WEC-type floating breakwater as one integrated WEC-type of breakwater system were raised by Ning et al. (2016). This paper focuses on further developing this system by adding dual floating bodies in this system. Some analytical studies have shown that the dual-floating body system has better performance than single-floating body system (Ning et al., 2017a). Future parametric study is implemented in this paper by numerical method based on OpenFOAM® which solves Navier-Stokes equations. Comparing to the analytical method, viscosity of the flow is considered in this research. Thus, the numerical results are expected to reflect real performance as similar as physical wave-structure interactions. Two parameters, including linear damping coefficient of PTO system λ_{PTO} and gap width between two floating bodies D, are investigated to show how they influence the performance of this hybrid system. Wave transmission factor K_T, which is defined as the ratio of the transmitted wave height to the incident wave height, is employed to evaluate the performance of wave attenuation. In addition, capture width ratio CWR, which is defined as the ratio of absorbed wave power to the incident wave power in the device width, is used to evaluate the efficiency of wave energy extraction. As for the overall evaluation of the multi-functional system, the range of effective frequency B_w, which is ranged with wave transmission factor K_T<0.5 and capture width ratio CWR>0.2, is obtained by the results of K_T and CWR and employed to evaluate performance, because breakwater is often considered as operating satisfactory when K_T<0.5, and the effective capture width ratio CWR for the wave energy converter should be greater than 20% (Ning et al., 2016). The improvements of this concept and future direction of developments are suggested by the analysis of K_T, CWR and B_w with variations of linear damping coefficient of PTO system λ_{PTO} and gap width between two floating bodies D.

2 NUMERICAL MODEL

For this study, the solver, *interDyMFoam* within OpenFOAM package, is employed for dynamic mesh to simulate fluid-floating structure interactions. Waves are generated and dissipated by using the relaxation-based wave generation toolbox *waves2Foam* proposed by Jacobsen et al. (2012). The Navier-Stokes equations, which is introduced below, are utilised for *interFOAM* and *interDyMFOAM* to describe the motion of fluid continuum. These

equations are written as a mass conservation equation and momentum equation by Newton's second law, which are showed below respectively:

$$\nabla \cdot \vec{U} = 0 \tag{1}$$

$$\frac{\partial \rho \vec{U}}{\partial t} + \nabla \cdot \left(\rho \vec{U}\vec{U}\right) - \nabla \cdot \left(\mu \nabla \vec{U}\right) - \rho \vec{\mathrm{g}} = -\nabla p - \overrightarrow{f_\sigma} \tag{2}$$

Where $\vec{U}$ is the flow velocity vector, ρ is the density of fluid, μ refers to the dynamic viscosity, $\vec{\mathrm{g}}$ is the acceleration of gravity, p is the pressure of fluid, and the last term $\overrightarrow{f_\sigma}$ is the surface tension which has minor effects in civil engineering issues. Thereinto, three components of the velocity vector in three dimensions of Cartesian coordinates and the fluid pressure are unknown variables in governing equations.

To track the shape and position of the free surface, the volume of fluid (VOF) method has been employed in OpenFOAM®. The transport equation of the VOF field can be yielded as:

$$\frac{\partial \gamma}{\partial t} + \nabla \cdot \left(\vec{U}\gamma\right) = 0 \tag{3}$$

Where, γ is the volume fraction. $\gamma = 0$ is for air, 1 is for water and intermedia value is for the mixture of two fluids at the interface. This equation shows the relationship between the velocity field and γ in each cell. While, in order to keep tracking accurate free surface, an additional convective is included in the transport equation to provide a sharper interface resolution. The velocity field is modelled by the corresponding gas and liquid velocities denoted by $\vec{U}_{\mathrm{g}}$ and $\vec{U}_{\mathrm{l}}$, respectively. The velocity field can be yielded by weighed averages as $\vec{U} = \gamma \vec{U}_{\mathrm{l}} + (1-\gamma)\vec{U}_{\mathrm{g}}$. According to this equation for velocity field, the new transport equation of VOF can be written as:

$$\frac{\partial \gamma}{\partial t} + \nabla \cdot \left(\vec{U}\gamma\right) + \nabla\left[\vec{U}_r \gamma(1-\gamma)\right] = 0 \tag{4}$$

Where $\vec{U}_r = \vec{U}_{\mathrm{l}} - \vec{U}_{\mathrm{g}}$. In the simulation of OpenFOAM®, two immiscible fluids are considered as one effective fluid throughout the flow domain. The physical properties, including density and dynamic viscosity, can be denoted as weighed averages by using volume fraction γ.

$$\phi = \gamma \phi_{water} + (1-\gamma)\phi_{air} \tag{5}$$

Based on this method, these physical properties can be equal to the properties of each fluid in their corresponding occupied regions and varying only across the interface.

3 NUMERICAL MODEL SETUP AND VALIDATION

The computational domain for the numerical simulations in this research is shown in Figure 1. The numerical simulations are in two-spatial domains. The wave depth is kept at $1m$. The computational domain is divided into three zones. The first zone is wave generation zone which is used to define and generate incident waves. This research focus only on regular wave interacting with the integrated system. Meanwhile, the wave generation zone is defined as a wave relaxation zone to dissipate the reflected waves from the structure, and the wave relaxation zone is set to $1.5L$ (Jacobsen et al., 2012), where L is the wave length. The second zone is wave-structure interaction zone. The pile-restrained WEC-type dual-floating system and wave gauges are installed in this zone. The hybrid system consists of two identical floating bodies. The parameters are shown in Figure 1. Because the test cases are 2D cases, the transverse lengths of these two floating bodies are defined as $0.02m$ which is the same as the transverse length of the computational domain. The definition of parameters including self-weight of the floating body and damping coefficients is based on the dimensions of the floating bodies. These floating bodies work as floating breakwaters and are restrained by the vertical piles, which make the floating bodies have heave motions only. The PTO system is connected with floating bodies to generate power, which applies linear damping on floating bodies with the damping coefficient λ_{PTO}. The two floating bodies are connected with one PTO system, which means that same damping is applied on the two floating bodies in each test. As for the calculation of *CWR*, the λ_{PTO} will be used to yield time-averaged damping forces F_{PTO} which is in the form of Coulomb damping force. The detailed description is given by Ning et al. (2016). The setup of the two wave gauges are shown in Figure 1 to measure the

transmitted wave height to calculate K_T. The third zone is a relaxation zone for absorbing transmitted waves. Similar to the wave generation zone, the length of the relaxation zone is set to 1.5L. As mentioned in the introduction, this study aims to investigate the influence of gap width and damping coefficient on the performance of this system. Thus, different gap widths are tested. And for each gap width, different damping coefficients and wave conditions are tested. The detailed description of test conditions is shown in Table 1.

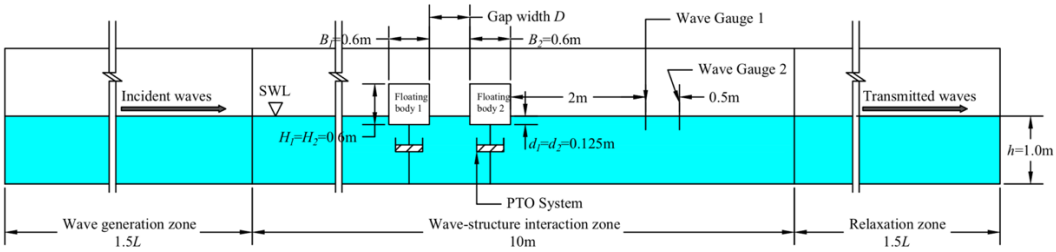

Figure 1. The computational domain of numerical wave tank and description of pile-restrained WEC-type dual-floating breakwater device (L is wave length).

Table 1. Variables considered in the test cases.

Wave height (m)	Wave period (s)	Damping coefficient ($N/(m/s)$)	Gap width (m)
0.12	0.95, 1.16, 1.37, 1.58, 1.79, 2.00, 2.21, 2.42	15, 25, 35, 45, 55	0.1, 0.2, 0.4, 0.6, 1.0

The validations of the numerical model use relevant experimental data collected in the wave tank in Dalian University of Technology (Ning et al., 2017b). The test conditions for the validation cases are shown in Table 2.

Table 2. Test conditions for the dual-pontoon system with B_1=B_2=0.6m, d_1=d_2=0.125m and D=0.2m. T is wave period, A is wave amplitude, k is wave number, h is water depth, kh is used to denote dimensionless wave number.

	T (s)	1.17	1.22	1.27	1.33	1.4	1.5	1.6	1.7
	A (m)	0.04	0.06	0.06	0.07	0.07	0.07	0.07	0.07
	kh	2.954	2.726	2.526	2.318	2.112	1.874	1.684	1.528
F_{PTO}	Case 1	9.92	33.04	39.87	50.12	60.83	57.56	59.66	58.88
(N)	Case 2	23.02	46.78	71.069	71.77	92.86	81.34	121.65	105.12

Two factors, K_T and CWR, are observed and compared in Figure 2, where the numerical results have achieved good agreements with experimental data. The numerical results well represent the trends of K_T and CWR as functions of kh. However, the value of K_T in numerical results are slightly smaller than that of experimental data and the value of CWR in numerical results are slightly higher than that of experimental data. This phenomenon may be because the tests by numerical simulations are in ideal states, while the experimental data may be influenced by friction loss. In sum, this numerical model shows good performance to simulate this pile-restrained WEC-type dual-floating breakwater system.

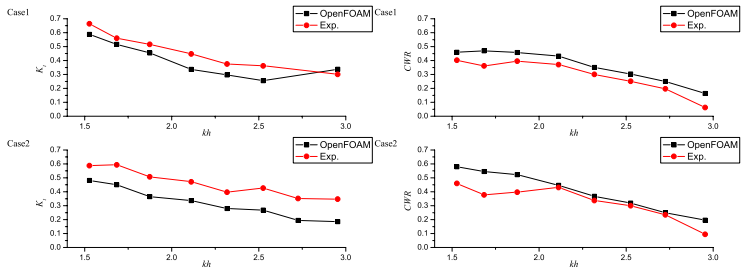

Figure 2. Comparison of wave transmission factor K_T and capture with ratio CWR between the experimental data and numerical results for Case 1 and Case 2

3 RESULTS AND DISCUSSIONS

Different cases with 5 groups of different gap widths are conducted in these numerical simulations by OpenFOAM®, the results of 3 groups are shown in Figure 3 to present the variations of K_T and *CWR* against different wave conditions, which are denoted by dimensionless wave number *kh*, in Case a to Case e which correspond to different gap widths D=0.1m, D=0.6m and D=1.0m respectively.

The K_T of all these cases shown in Figure 3 generally decreases with the increase of *kh*. Meanwhile, the K_T *vs. kh* curves in Figure 3 show that the K_T has the general tendency to decrease with the increase of damping coefficients of PTO system. However, the decrease is not significant. That means the changes of damping coefficient λ_{PTO} have minor influences on the K_T. As for the *CWR*, the curves of *CWR vs. kh* in Figure 3 show that peak point of the *CWR* curves happens at different *kh* for different damping coefficients, and after the peak point, the *CWR* decreases with the increase of *kh*. However, there is an oscillation in *CWR* curves of Case d and e due to Bragg reflection (Garnaud and Mei, 2009; Ouyang et al., 2015). According to the analytical results (Ning et al., 2017a), the oscillation will occur at high frequency region and it will tend to occur at lower frequency with the increase of gap width. According to Figure 3, the range of effective frequency can be obtained, more detailed discussions will be presented at the Workshop.

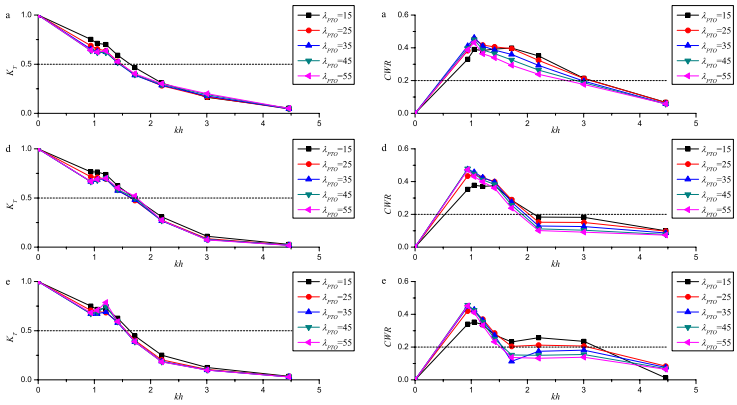

Figure 3. The variations of K_T and *CWR* against dimensionless wave number, *kh*, for different damping coefficients (λ_{PTO}, Unit: *N/(m/s)*) of PTO system in Case a, Case d and Case e.

ACKNOWLEDGEMENT

The authors thank UK Royal Academy of Engineering and EPSRC for providing partial support for this work within the RAE UK-CIAPP (RAE Grant No. UK-CIAPP/73) and EPSRC project ResIn (EPSRC Grant No. EP/R007519/1).

REFERENCES

Garnaud, X. and Mei, C., 2009. Bragg scattering and wave-power extraction by an array of small buoys. *Proceeding of the royal society A: Mathematical, Physical and Engineering Sciences* October 02, 2009, 466, pp. 79-106.

Jacobsen, N.G., Fuhrman, D.R., Fredsøe, J., 2012. A wave generation toolbox for the opensource CFD library: OpenFoam®. Int. J. Numer. Meth. Fluids., 70, pp.1073–1088.

Ning, D., Zhao, X., Goteman, M. and Kang, H., 2016. Hydrodynamic performance of a pile-restrained WEC-type floating breakwater: An experimental study. *Renewable Energy*, 95, pp.531-541.

Ning, D., Zhao, X., Zhao, M., Hann, M. and Kang, H., 2017. Analytical investigation of hydrodynamic performance of a dual pontoon WEC-type breakwater. *Applied Ocean Research*, 65, pp. 102-111

Ning, D., Zhao, X., Zang, J. and Johanning, L., 2017b. Analytical and experimental study on tandem WEC-type floating breakwaters. *12th European Wave and Tidal Energy Conference*, 27 August - 1 September 2017, Cork. Cork: EWTEC.

Ouyang, H., Chen, K. and Tsai, C., 2015. Investigation on bragg reflection of surface water waves induced by a train of fixed floating pontoon breakwaters. *Int. J. Nav. Archit. Ocean Eng* 7, pp. 951-963.